SUPPLEMENTARY DATA

fMRI Data Acquisition

Images were obtained using a 3-T Siemens Trio MRI system equipped with a standard quadrature head coil, using T2*-sensitive gradient-recalled single shot echo planar pulse sequence. Adolescents were positioned in the coil and head movements were minimized using foam pillows. After a 3-plane localizer, a high resolution 3D volume was collected using a Magnetization Prepared Rapid Gradient Echo (MPRAGE) sequence (176 contiguous sagittal slices, TR=2530 ms; echo time (TE)=2.4 ms; bandwidth=238 Hz/pixel; flip angle (FA)= 9°; slice thickness=1mm; field of view=256 x 256 mm; matrix=256 x 256). Next, a T1-weighted anatomical scan (TR=300 ms; TE=2.46 ms; bandwidth=310 Hz/pixel; FA= 60°; slice thickness=4mm; FOV=220 x 220 mm; matrix=256 x 256) was collected with 32 axialoblique slices parallel to the anterior and posterior commissure (AC–PC). After these structural images, six functional data series were then acquired with the same slice localizations as the axialoblique T1-weighted image. Functional image were collected using a T2* sensitive gradient-recalled single-shot echo-planar pulse sequence (TR=2000 ms; TE=25 ms; bandwidth=2520 Hz/pixel; FA=85°; slice thickness=4mm; FOV=220 x 220 mm; matrix=64 x 64; images per slice=198). Stimuli were projected onto a semi-transparent screen at the head of the bore, viewed by the subject via a mirror mounted on the head coil.

fMRI Data Preprocessing

All data were converted from Digital Imaging and Communication in Medicine (DICOM) format to analyze format using XMedCon (1). During the conversion process, the first three images of each run were discarded to enable the signal to achieve steady-state equilibrium between radio frequency pulsing and relaxation leaving 195 images per slice for analysis. Functional images were slice time corrected using sinc interpolation and motion corrected using SPM5 (www.fil.ion.ucl.ac.uk/spm/software/spm5) for three translational directions (x, y or z) and three possible rotations (pitch, yaw or roll). Trials with linear motion that had a displacement in excess of 1.5 mm or rotation in excess of 2° were rejected. All further analyses were performed using BioImage Suite (http://bioimagesuite.org). Individual subject data was analyzed using a General Linear Model (GLM) on each voxel in the entire brain volume with regressors specific for each task, High-calorie food (HCF), Low-calorie food (LCF), and Non-food (NF) with drift parameters regressed from the data (mean, linear and quadratic). The resulting output images for each task were normalized beta-maps, which were in the acquired space (3.438mm x 3.438mm x 4mm) and were spatially smoothed with a 6 mm Gaussian kernel to account for variations in the location of activation across subjects.

Image Registrations

To take these data into a common reference space, three registrations were calculated within the Yale BioImage Suite software package (http://www.bioimagesuite.org/(2)). The first registration performed a linear registration between the individual subject’s raw functional image and that subject's 2D anatomical image. The 2D anatomical image was then linearly registered to the individual's 3D anatomical image. The 3D differs from the 2D in that it has a 1×1×1 mm resolution whereas the 2D z-dimension is set by slice-thickness and its x-y dimensions are set by voxel size. Finally, a non-linear registration was computed between the individual 3D anatomical image and a commonly used 3D reference image (the Colin Brain (3) in MNI space (4)). All three registrations were applied sequentially to the individual normalized beta-maps to bring all data into the common reference space.

Supplementary Figure 1. Insulin resistance and leptin levels in the Obese and Lean groups. The Obese adolescents demonstrate a wide spectrum of (a) leptin levels, (b) insulin levels, (c) insulin resistance (assessed by WBISI) with statistically significant differences between the two groups.

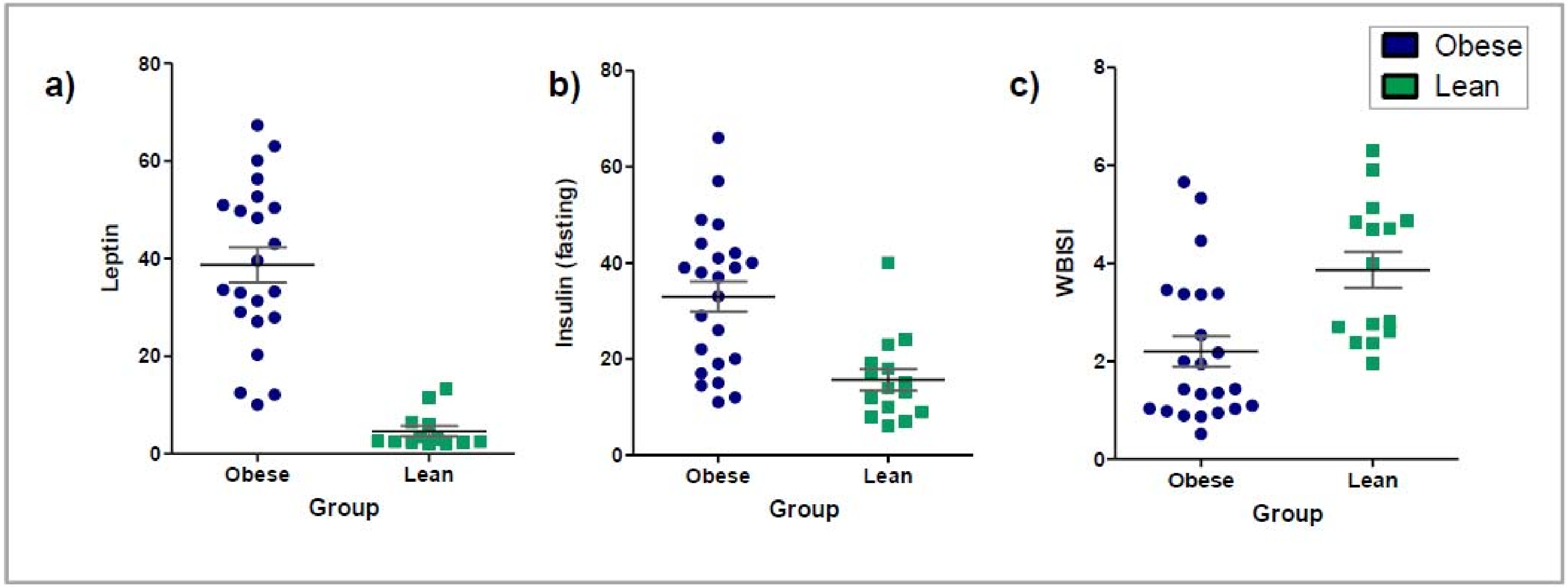

Supplementary Figure 2. Liking and wanting in Obese and Lean groups. Subjective liking and wanting ratings for HCF, LCF, and NF pictures presented during the fMRI session were not different in Obese as compared to Lean adolescents. There were statistically significant differences between condition response (Wanting: HCF vs. NF $p<0.0001$, HCF vs. LCF $p=0.0001$, LCF vs NF $p=0.0013$; Liking: HCF vs. NF $p<0.0001$, HCF vs. LCF $p<0.0001$, LCF vs. NF $p=0.023$).

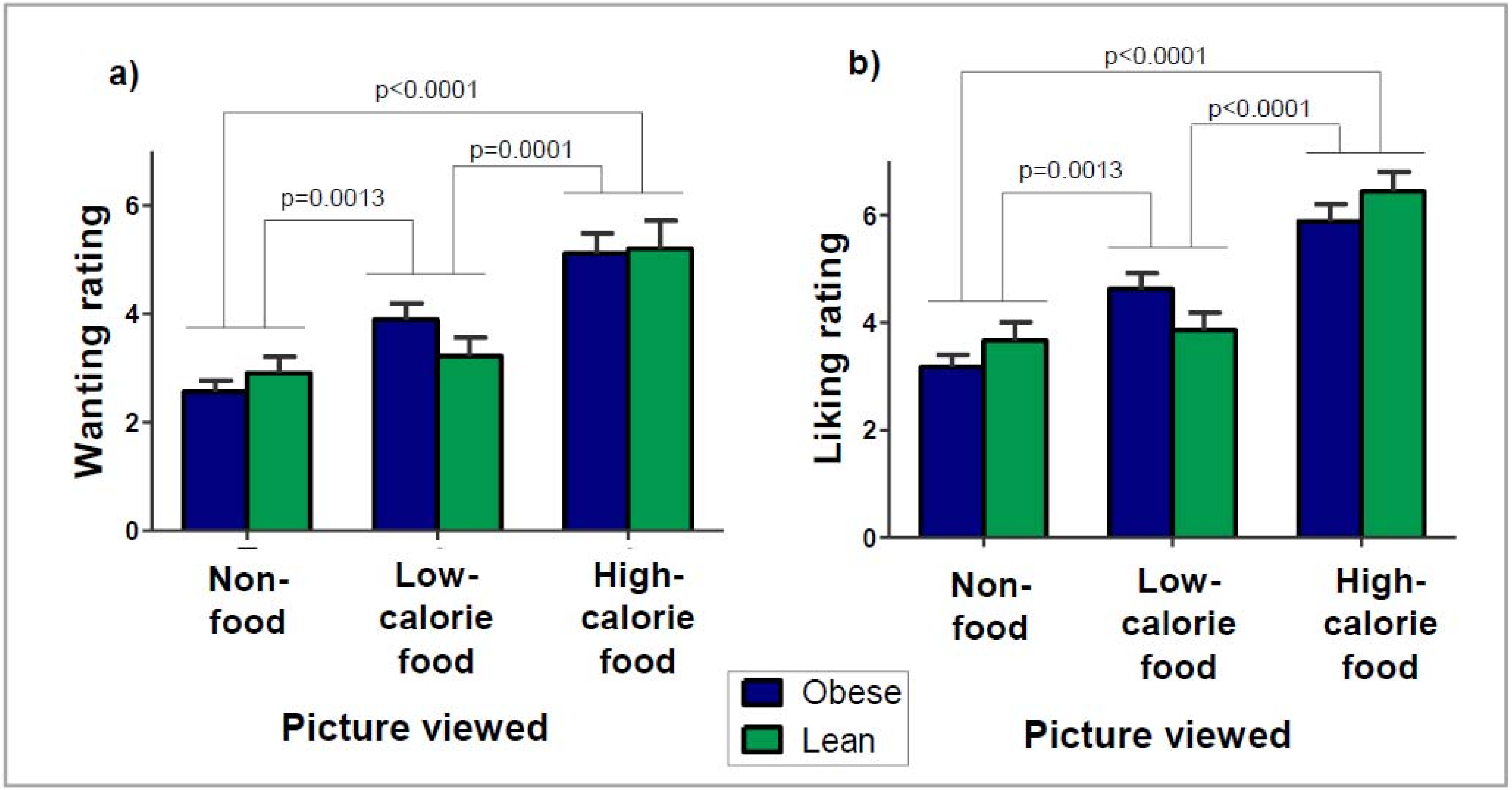

SUPPLEMENTARY DATA

Supplementary Figure 3. Within-group neural response differences in cue condition contrasts. Axial brain slices of neural activation differences in low-calorie food vs non-food in (a) Obese (b) Lean (c) Obese compared to Lean adolescents (threshold of p<0.05, FWE-corrected). R, right; L, left; FWE, family-wise-error. Talairach z-levels indicated.

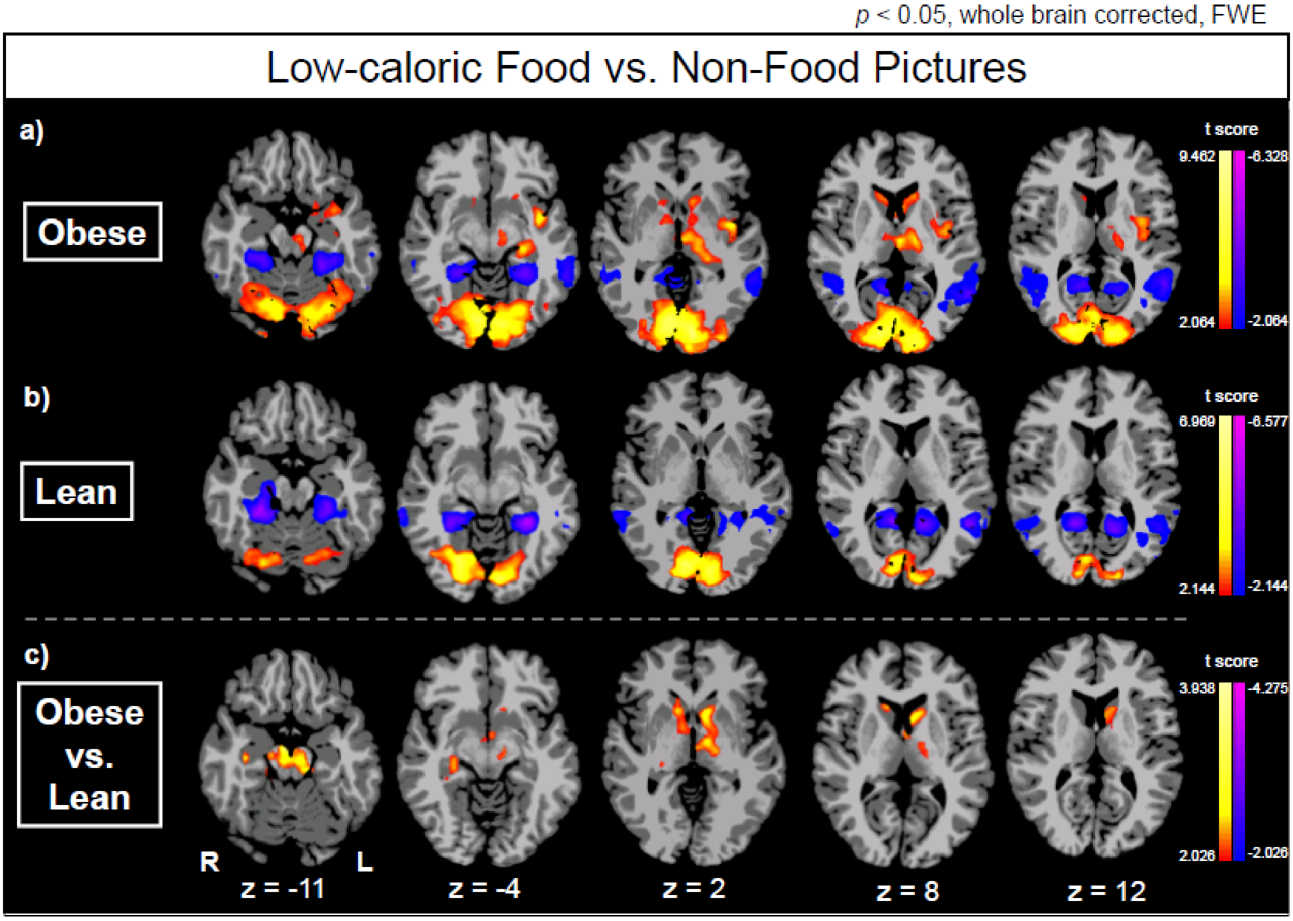

SUPPLEMENTARY DATA

Supplementary Figure 4. Within-group neural response differences in cue condition contrasts covaried for age, sex, and race. Axial brain slices of neural activation differences in high-calorie food vs. non-food in Obese compared to Lean adolescents (threshold of $p<0.05$, FWE-corrected). R, right; L, left; FWE, family-wise-error. Talairach z-levels indicated.

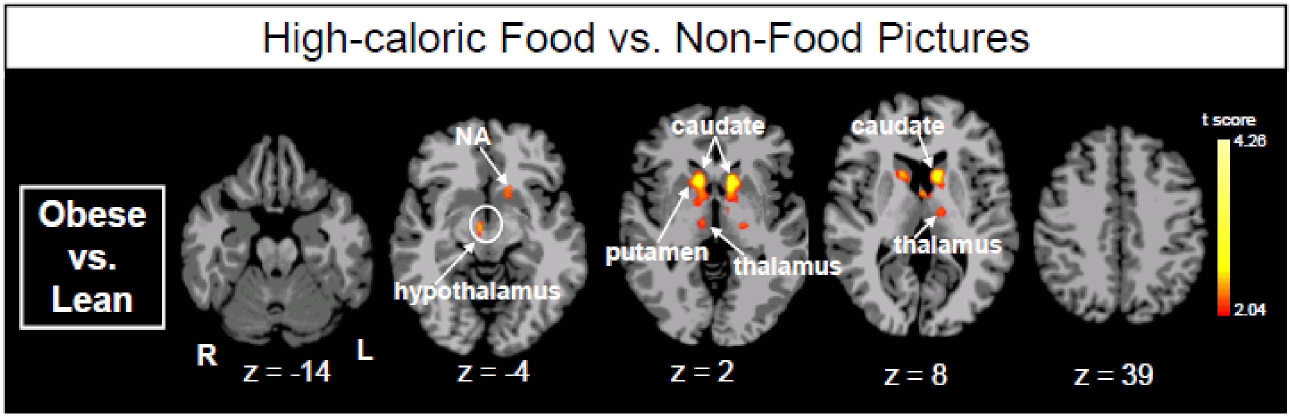

Supplementary Figure 5. Beta-weight (BOLD signal) extracted from regions of interest (ROIs). There were no statistically significant differences between the Obese-IR and Obese-IS groups in terms of BOLD signal response in the identified regions of interest. There were statistically significant differences between the Obese-IR vs. Lean and the Obese-IS vs Lean groups in each of the ROIs. P<0.05, whole brain corrected ROIs.

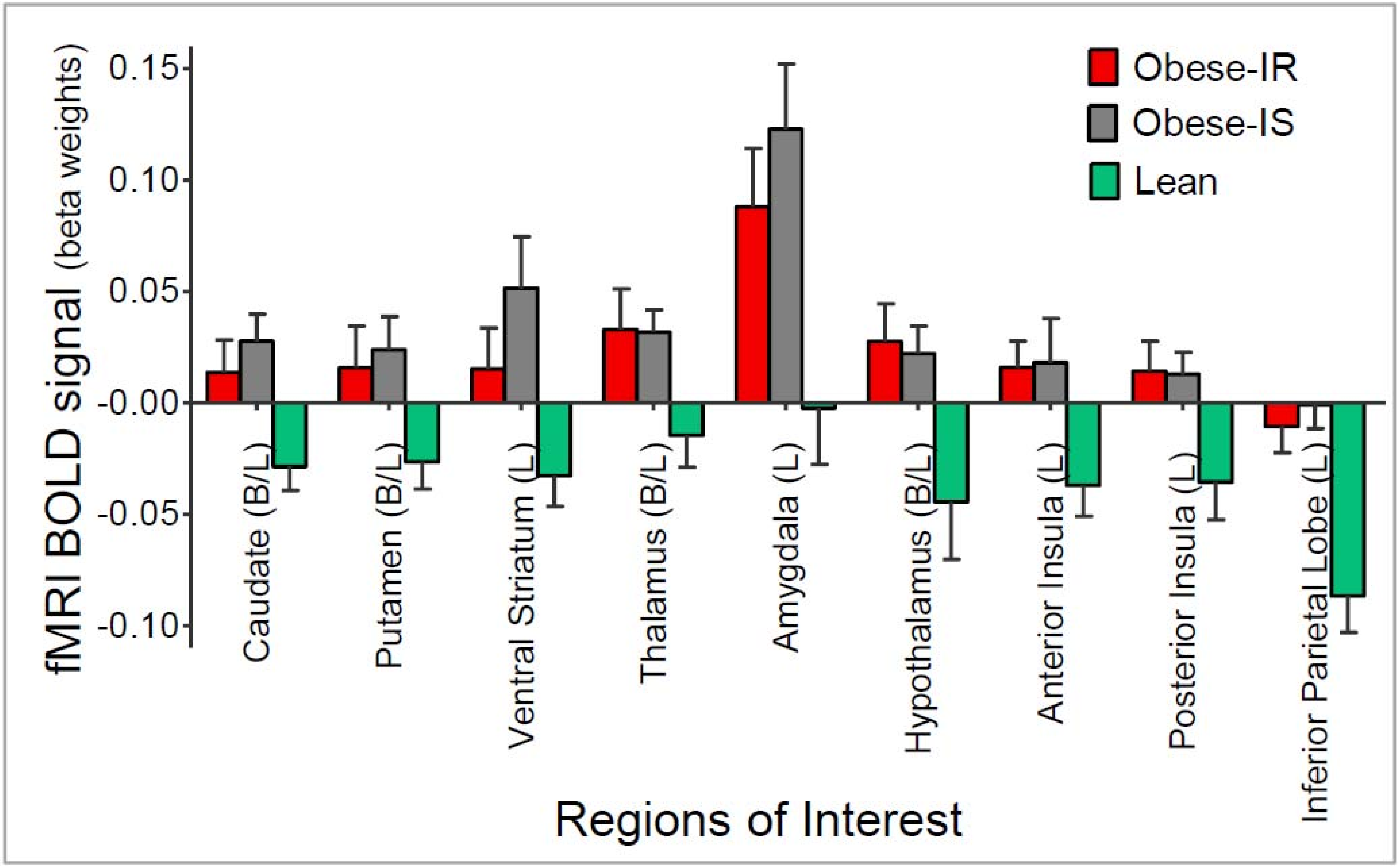

SUPPLEMENTARY DATA

Supplementary Table 1. Regional brain activation. Observed in between-condition contrast A) High-calorie food vs. Non-food, B) Low-calorie food vs. Non-food, C) High-calorie food vs. Low-calorie food.

(A) High-calorie food vs. Non-food (p=0.05)

Obese vs. Lean adolescents	Broadmann Area	Laterality	Volume (mm^3)	Vol (voxels)	Coordinates (Center Mass)	Mean T-Value	d (effect size)
Caudate, thalamus, putamen, nucleus accumbens, insula, amygdala, and hypothalamus		bilateral	13911	515.2222222	-6,1,2	2.38	0.532188457
Amygdala		*left*	*546*	*20.22222222*	*-23,0,-14*	*2.409*	0.538673107
Ventral striatum		*left*	*160*	*5.925925926*	*-13,8,-7*	*2.421*	0.54135641
Hypothalamus		*bilateral*	*422*	*15.62962963*	*1,-4,-3*	*2.269*	0.507367903
Caudate		*bilateral*	*3141*	*116.3333333*	*-5,11,5*	*2.589*	0.578922654
Anterior Insula		*left*	*171*	*6.333333333*	*-32,10,-10*	*2.332*	0.521455245
Thalamus		*bilateral*	*1602*	*59.33333333*	*-8,-18,7*	*2.195*	0.490820867
Putamen		*bilateral*	*830*	*30.74074074*	*5,5,2*	*2.245*	0.502001297
Hippocampus, primary auditory cortex, and primary motor cortex	6,44,47	left	7041	260.7777778	-43,-10,3	2.344	0.524138548
Posterior Insula		*left*	*907*	*33.59259259*	*-38,-20,8*	*2.327*	0.520337202
Whitematter	40	right	9584	354.962963	21,-29,23	2.357	0.52704546
Primary sensory cortex, primary motor cotex	39,40	left	12137	449.5185185	-47,-49,33	2.595	0.580264305
Inferior Parietal Lobe		*left*	*10895*	*403.5185185*	*-47,-52,33*	*2.638*	0.589879475

Obese adolescents	Broadmann Area	Laterality	Volume (mm^3)	Vol (voxels)	Coordinates (Center Mass)	Mean T-Value	d (effect size)
Fusiform, cerebellum, brainstem, thalamus, caudate, hippocampus, amygdala, insula	17,18,19	bilateral	156804	5807.555556	-1,-62,-2	3.348	0.6696
Hippocampus, amygdala, insula		right	11633	430.8518519	28,-12,-7	2.817	0.5634
Middle and superior temporal gyrus	21,22,39	left	15678	580.6666667	-49,-54,15	-2.639	-0.5278
Fusiform gyrus	19,22,39	right	11611	430.037037	48,-53,20	-2.614	-0.5228
Posterior cingulate, primary motor cortex, and primary sensory cortex	6,7,8,9	bilateral	51499	1907.37037	13,-34,39	-2.7	-0.54
Primary sensory and primary motor cortex	6,7,40	left	7375	273.1481481	-40,-27,50	2.877	0.5754

Lean adolescents	Broadmann Area	Laterality	Volume (mm^3)	Vol (voxels)	Coordinates (Center Mass)	Mean T-Value	d (effect size)
Parahippocampus, fusiform gyrus, anterior and posterior cingulate, primary sensory, motor, and auditory cortex	6,8,9,18,19,20,21,22,38,39,4	bilateral	244213	9044.925926	5,-29,25	-2.866	-0.640862235
Primary visual cortex and cerebellum	18	bilateral	59575	2206.481481	0,-78,0	3.41	0.762505311
Primary auditory cortex	10,44,45,47	left	12002	444.5185185	-41,16,4	-2.747	-0.614252812

(B) Low-calorie food vs. Non-food (p=0.05)

Obese vs. Lean adolescents	Broadmann Area	Laterality	Volume (mm^3)	Vol (voxels)	TalCoordCenterMass	Mean T-Value	d (effect size)
Caudate, thalamus, brainstem, hippocampus, and hypothalamus		bilateral	13771	510.037037	0,-12,-4	2.261	0.505579034
Caudate		*left*	*2025*	*75*	*-11,8,6*	*2.297*	0.513628944
Caudate		*right*	*699*	*25.88888889*	*10,13,1*	*2.188*	0.489255607
Thalamus		*left*	*1263*	*46.77777778*	*-11,-13,4*	*2.268*	0.507144295
Hypothalamus		*left*	*136*	*5.037037037*	*-3,-5,-5*	*2.206*	0.493280562
Hypothalamus		*right*	*75*	*2.777777778*	*4,-8,-6*	*2.098*	0.469130833
Hippocampus		*right*	*1072*	*39.7037037*	*30,-26,-6*	*2.249*	0.502895731

Obese adolescents	Broadmann Area	Laterality	Volume (mm^3)	Vol (voxels)	TalCoordCenterMass	Mean T-Value	d (effect size)
Posterior cingulate, fusiform gyrus	7,18,19	bilateral	43052	1594.518519	0,-51,19	-2.827	-0.5654
Hippocampus, amygdala, insula, putamen, caudate, thalamus, brainstem		left	20898	774	-19,-9,0	2.656	0.5312
Fusiform gyrus	19,21,39	left	18708	692.8888889	-49,-55,12	-2.777	-0.5554
Fusiform gyrus, cerebellum	17,18,19	bilateral	72420	2682.222222	0,-79,0	3.561	0.7122
Fusiform gyrus	19,21,39	right	10108	374.3703704	47,-57,15	-2.545	-0.509
Anterior cingulate, primary sensory and primary motor cortex	6	right	13273	491.5925926	33,-19,50	-2.607	-0.5214

Lean adolescents	Broadmann Area	Laterality	Volume (mm^3)	Vol (voxels)	TalCoordCenterMass	Mean T-Value	d (effect size)
Parahippocampus, posterior cingulate, and fusiform gyrus	19	right	14676	543.5555556	19,-41,0	-3.092	-0.798351038
Fusiform gyrus, posterior cingulate gyrus	18,19,39	left	28722	1063.777778	-35,-54,12	-2.828	-0.730186525
Fusiform gyrus, cerebellum	17,18,19	bilateral	30244	1120.148148	4,-78,0	3.051	0.787764883
Fusiform gyrus	19,21,39	right	9837	364.3333333	52,-59,20	-2.575	-0.664862201

(C) High-calorie food vs. Low-calorie food (p=0.05)

Obese vs. Lean adolescents	Broadmann Area	Laterality	Volume (mm^3)	Vol (voxels)	TalCoordCenterMass	Mean T-Value	d (effect size)
none							

Obese adolescents	Broadmann Area	Laterality	Volume (mm^3)	Vol (voxels)	TalCoordCenterMass	Mean T-Value	d (effect size)
Hippocampus, parahippocampus, amygdala, cerebellum, and fusiform gyrus	7,18,19,39	bilateral	79699	2951.814815	6,-54,-2	2.705	0.541
Visual cortex, anugular gyrus, sensory association cortex	7,19,39	left	7503	277.8888889	-26,-64,36	2.512	0.5024

Lean adolescents	Broadmann Area	Laterality	Volume (mm^3)	Vol (voxels)	TalCoordCenterMass	Mean T-Value	d (effect size)
Hippocampus, hypothalamus, parahippocampus, and fusiform gyrus		right	7818	289.5555556	29,-36,-9	2.708	0.699202656

Supplementary Table 2. Correlations with Leptin in all subjects with whole brain corrected brain maps. Correlation in the following regions: a) hypothalmus, b) caudate, c) amygdala, d) hippocampus, e) parahippocampus, f) anterior insula.

	Broadmann Ar	Laterality	Volume (mm^3)	Vol (voxels)	Coordinates (Center Mass)
Caudate, putamen, insula, thalamus, hippocampus, amygdala, brain stem, cerebellum, posterior and anterior cingulate gyrus, auditory and primary motor cortex	6,7		71339	2642.185185	0,-27,5
Hypothalamus			*573*	*21.22222222*	*0,-4,-1*
Caudate			*3726*	*138*	*-5,11,7*
Putamen			*1551*	*57.44444444*	*-11,2,1*
Thalamus			*1023*	*37.88888889*	*-15,-17,5*
Hippocampus			*2711*	*100.4074074*	*4,-18,-11*
Amygdala			*791*	*29.2962963*	*-6,-2,-16*
Parahippocampus			*3299*	*122.1851852*	*1,-33,-6*
Anterior insula			*321*	*11.88888889*	*-29,8,-10*
Posterior insula			*991*	*36.7037037*	*-34,-22,7*
Posterior cingulate			*4810*	*178.1481481*	*-1,-47,32*
Angular Gyrus	39	left	6290	232.962963	-46,-58,31

SUPPLEMENTARY DATA

References

1. Nolf E: XMedCon - An open-source medical image conversion toolkit. European Journal of Nuclear Medicine 2003;Vol. 30:pp S246

2. Joshi A, Scheinost D, Okuda H, Belhachemi D, Murphy I, Staib LH, Papademetris X: Unified framework for development, deployment and robust testing of neuroimaging algorithms. Neuroinformatics 2011;9:69-84

3. Holmes CJ, Hoge R, Collins L, Woods R, Toga AW, Evans AC: Enhancement of MR images using registration for signal averaging. Journal of computer assisted tomography 1998;22:324-333

4. Evans AC, Collins DL, Mills SR, Brown ED, Kelly RL, Peters TM: 3D statistical neuroanatomical models from 305 MRI volumes. Proc IEEE Nucl Sci Symp Med Imaging Conf 1993:pp. 1813–1817